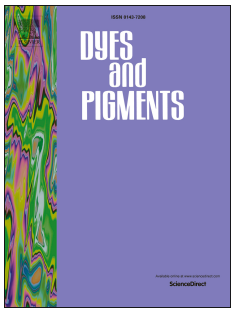

A novel dual-function bithiophene-Meldrum's acid based chemosensor for highly sensitive, colorimetric and fluorimetric detection of cyanide and hypochlorite and its applications

Chunpeng Li, Qingfen Niu, Tianduo Li, Tao Wei, Tingting Hu, Jianbin Chen, Xuyang Qin, Lan Yang

PII: S0143-7208(20)30463-0

DOI: https://doi.org/10.1016/j.dyepig.2020.108459

Reference: DYPI 108459

To appear in: *Dyes and Pigments*

Received Date: 19 February 2020

Revised Date: 1 April 2020

Accepted Date: 19 April 2020

Please cite this article as: Li C, Niu Q, Li T, Wei T, Hu T, Chen J, Qin X, Yang L, A novel dual-function bithiophene-Meldrum's acid based chemosensor for highly sensitive, colorimetric and fluorimetric detection of cyanide and hypochlorite and its applications, *Dyes and Pigments* (2020), doi: https://doi.org/10.1016/j.dyepig.2020.108459.

Author contributions

Chunpeng Li: Conceptualization, Data curation, Software, Investigation, Writing-Original Draft.

Lan Yang: Validation, Formal analysis, Visualization.

Qingfen Niu: Resources, Writing-Review & Editing, Supervision, Data Curation.

Tianduo Li: Resources, Formal analysis, Review & Editing.

Tao Wei: Formal analysis, Review & Editing.

Tingting Hu: Formal analysis, Review & Editing.

Jianbin Chen: Review & Editing.

Xuyang Qin: Review & Editing.

Graphical Abstract

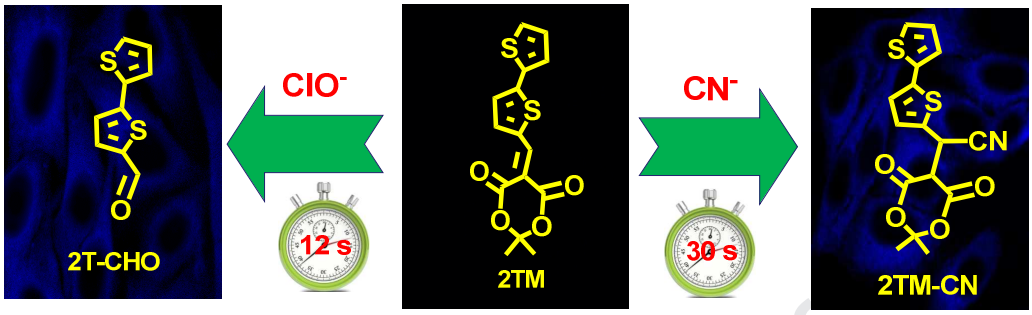

A novel dual-function bithiophene-Meldrum's acid based chemosensor for highly sensitive, colorimetric and fluorimetric detection of cyanide and hypochlorite and its applications

Chunpeng Li, Qingfen Niu*, Tianduo Li, Tao Wei, Tingting Hu, Jianbin Chen, Xuyang Qin, Lan Yang

Shandong Provincial Key Laboratory of Molecular Engineering, School of Chemistry and Pharmaceutical Engineering, Qilu University of Technology (Shandong Academy of Sciences), Jinan 250353, People's Republic of China

Abstract

A dual-function bithiophene-Meldrum's acid based chemosensor **2TM** was developed, which displayed ultrafast, colorimetric and fluorescence turn-on responses for CN^- and ClO^- with specific selectivity and high sensitivity. The sensor **2TM** for CN^- detection in DMSO/H_2O (1/3, V/V) solution was based on the nucleophilic addition of CN^- to sensor, which resulted in remarkable spectral and discernable color changes. Meanwhile, **2TM** showed specific selectivity for ClO^- in 100% aqueous solution based on the sensing mechanism of oxidative cleavage of C=C bond. The detection limits were obtained to be 0.96 μM for CN^- and 48 nM for ClO^-. The sensing mechanism of **2TM** toward CN^- and ClO^- was investigated by job'plot, FTIR, ^{1}H NMR, HRMS and optical spectra. The sensor **2TM** loaded colorimetric test strips/supported silica measurements demonstrated to be a portable, eco-friendly and ultrafast device for real-time and on-site visual detection of CN^- and ClO^- in water by the naked eye. More importantly, sensor **2TM** with excellent photophysical properties and low biotoxicity was successfully applied to detect CN^- and ClO^- in live cells and environmental water samples, as well as capable of monitoring CN^- in the natural food samples, illustrating its practical utility in biological and environmental systems.

Keywords: Chemosensor; Hypochlorite; cyanide; Bithiophene-Meldrum's acid; Bioimaging; Test strip.

* To whom the correspondence should be addressed
E-mail: qf_niu1216@qlu.edu.cn
Telephone: +86(531)89631760
Fax number: +86(531)89631208

1. Introduction

Cyanide (CN^-) as a powerful poison is highly toxic to human health even at an extreme low concentration [1-2]. However, cyanide-containing compounds are widely used in the chemical and industrial processes, such as synthetic plastic and resin industry, the production of pharmaceuticals and pesticides, consumption of certain foods, metallurgy, electroplating and gold/silver mining [3-6]. The extensive exposure of poisonic cyanide anion to the environment and water source can cause various serious health problems such as damage to the central nervous system and visual nervous system, disturbance of metabolism, inhibition of respiration and even death ascribed to its blocking the electron transport chain and inhibiting cellular respiration [7,8]. Accordingly, the World Health Organization (WHO) regulates the specified limit of cyanide in drinking water to be 1.9 μM [9]. Therefore, an efficient method to rapidly and precisely detect trace CN^- in environmental and biological systems is of great significance to human health and environment protection.

Hypochlorite (ClO^-) is one of the most important reactive oxygen species (ROS) in living organisms, which particularly participates in various physiological and pathological processes and can react with many biological molecules in living organisms including DNA, RNA, cholesterol, fatty acids, and a variety of proteins [10-15]. Besides, due to its strong oxidation ability,

ClO^- is also widely used as an indispensable disinfectant, household bleach and antimicrobial agent in our daily life [16-18]. Endogenous ClO^- is mainly produced by myeloperoxidase-catalysed reaction between H_2O_2 and Cl^-, and it is generally considered as an important antimicrobial agent in the immune system to defense the invasive bacterial pathogens [19]. However, excessive ClO^- will increase oxidative stress, and resulting in tissue damage and various diseases such as lung injury, nephrosis, neurodegeneration, atherosclerosis, cancer, Alzheimer's and cardiovascular diseases [20,21]. Consequently, it is highly desirable to develop a reliable analytical method for real-time monitoring of ClO^- in environmental and biological systems.

Optical sensor technique with outstanding fluorescence and color changes has been confirmed to be the most convenient and popular analytical method for efficient identification of various cations, anions and biomolecules [22-37]. Compared with the electroanalysis, potentiometry and ion chromatography, reaction-based fluorescent sensor as a promising tool for the recognition of various analytes has garnered tremendous attentions because of its unique selectivity, excellent sensitivity, visualization, facile operation, no damage, reliability, real-time imaging, fast response and usability to biological system [38-42]. Recently, a numerous reaction-based fluorescent sensors have been exploited to detecting CN^- and ClO^- [43-52], which shows better selectivity and can effectively avoid interference of other

tested species. However, some of them could only detect one single CN^- or ClO^- anion, which significantly limited their application. In contrast, the multi-function fluorescent sensor which could detect multiple targets based on different mechanisms displayed many unique advantages of simple operation and multiplicity. Therefore, developing simple and water-soluble fluorescent sensors with good capability of detecting more than one target in enviro/biological systems has gained increasing attention. Unfortunately, only two fluorescent sensors have been reported for simultaneous detection of CN^- and ClO^- [53-55]. As a result, it is particularly urgent to develop dual-function fluorescent sensors to quickly, accurately and simultaneously detect CN^- and ClO^- in biological and environmental samples with excellent sensitivity and selectivity, which is of significant importance for scientific investigations, pollution monitoring and medical diagnosis.

Herein, we synthesized a simple dual-function bithiophene-Meldrum's acid based colorimetric and fluorescent turn on sensor **2TM** (**Scheme 1**) for the specific and sensitive simultaneously detection of CN^- and ClO^- through different sensing mechanisms. Sensor **2TM** in aqueous media exhibited excellent specificity for CN^- and ClO^- with visible naked-eye changes, and could quantitatively and sensitively detect CN^- and ClO^- with low detection limits of 0.96 μM and 48 nM, respectively. Moreover, excellent recognition properties of **2TM** with good water dispersibility, ultrarapid response (CN^-

< 30 s, ClO^- < 12 s), specific selectivity, great sensitivity, and admirable cell permeability were exhibited, which made the sensor **2TM** act as a promising tool to monitor CN^- and ClO^- in the live cells, environmental water and the natural food analysis. Furthermore, the sensor **2TM** loaded colorimetric test strips/supported silica measurements further demonstrated to be a portable, eco-friendly and ultrafast device for real-time and on-site visual detection of CN^- and ClO^- in water. To the best of our knowledge, our developed sensor **2TM** is the fourth example to be successfully used for simultaneous detection of CN^- and ClO^- with ultrafast response and great sensitivity.

Scheme 1

2. Experimental Section

2.1 Instruments and reagents

The spectra of UV-Vis absorption, fluorescence, FTIR, NMR and HRMS were recorded using Shimadzu UV-2600 spectrophotometer, Hitachi F-4600 spectrophotometer, Bruker ALPHA FT-IR spectrometer, Bruker Advance II 400 MHz instruments and Agilent 6510 Accurate-Mass Q–TOF LC/MS system, respectively. The pH values were conducted by PHS-25 pH meter. MTT assay and fluorescence images were obtained using the microplate reader (MultiskanTM FC Microplate Photometer, Thermo

Scientific, USA) and Leica TCS SP8 confocal laser scanning microscope (CLSM) with a 63x magnification target oil lens, respectively. All chemical reagents and solvents were purchased from commercial suppliers of analytical reagent grade and were used directly without further purification unless otherwise stated. Deionized water was used throughout the test process. Compounds **2T** and **2T-CHO** were prepared by the previously reported procedures [56,57].

*2.2 Synthesis of sensor **2TM***

A mixture of compound **2T-CHO** (388 mg, 2.0 mmol) and Meldrum's acid (288 mg, 2.0 mmol) in dry 15 mL EtOH was added 2 drops of acetic acid glacial as catalyst. The reaction mixture was stirred for overnight under reflux. The resulting mixed solution was placed in the refrigerator overnight, and the precipitated solid was suction filtered washed with ethanol and dried in vacuum to give pure compound **2TM** as an orange red solid (325 mg, yield 83.5%). ^{1}H NMR (400 MHz, DMSO-d_6, ppm): δ = 8.64 (s, 1H), 8.25 (d, J = 4.0 Hz, 1H), 7.80 (d, J = 4.0 Hz, 1H), 7.72 (d, J = 4.0 Hz, 1H), 7.66 (d, J = 4.0 Hz, 1H), 7.24 (t, J = 4.0 Hz, 1H), 1.72 (s, 6H) (**Fig. S1**); ^{13}C NMR (100 MHz, DMSO-d_6, ppm): δ = 162.60, 161.15, 151.86, 148.40, 148.09, 135.21, 134.16, 129.50, 129.19, 127.68, 127.59, 125.06, 105.30, 104.41, 26.85 (**Fig. S2**); FTIR (KBr, cm^{-1}): ν = 3077 (C-H), 1717 (O-C=O),

1558 (C=C) (**Fig. S3**); HRMS (ESI): m/z calcd for $C_{15}H_{12}O_4S_2$ $[M + Na]^+$: 343.0075, found: 343.0062 (**Fig. S4**).

2.3 General spectroscopic procedures

Stock solution of the **2TM** (1.0 mM) was prepared in DMSO. A series of stock solutions of various anions (10 mM) and ROS including Br^-, F^-, Cl^-, CO_3^{2-}, HCO_3^-, PO_4^{3-}, SO_4^{2-}, HSO_3^-, SCN^-, AcO^-, NO_3^-, NO_2^-, ClO_4^-, ClO_3^-, ClO_2^-, I^-, H_2O_2, ROO• and O_2^- were dissolved in deionized water and used freshly. ROO• was obtained from 2,2'-azobis(isobutyramidine) dihydrochloride. The test solution of 10 μM **2TM** was prepared through pipetted out **2TM** stock solution (0.01 mL, 1.0 mM) into a volumetric flask with 100 mL deionized water and diluted to an appropriate concentration. All fluorescence and UV-Vis spectra of **2TM** were measured at room temperature. The fluorescence spectra were obtained under the condition of an excitation wavelength of 350 nm and slit widths of 5 nm/5 nm.

2.4 Live cell imaging

HeLa cells seeded in 96-well plates were incubated in DMEM medium with 10% fetal bovine serum (FBS) for 24 h (37 ^oC, 5% CO_2). For fluorescence imaging, these well-grown cells were treated with sensor **2TM** (15 μM) for 60 min and then washed with PBS buffer for three times. Subsequently, the **2TM**-treated cells were cultured with 20 μM ClO^-/CN^-

for 30 min, respectively, and then being washed three times with PBS buffer. The fluorescence images of the HeLa cells were measured with an CLSM under blue channel (430–470 nm) upon an excitation at 350 nm.

3. Result and Discussion

*3.1 Spectroscopic response of **2TM** towards CN^-*

The UV-Vis absorption and fluorescence spectral response of **2TM** towards CN^- was firstly investigated in DMSO/H_2O (1/3, V/V) solution. As displayed in **Fig. 1a**, after adding the CN^- (2.0 equiv.) to the **2TM** (10 μM), the strong absorption band at 452 nm disappeared and a new absorption band appeared at 315 nm, along with an immediate dramatic solution color change from yellow to colorless by the naked eyes. While, the other anions and ROS (Br^-, F^-, Cl^-, CO_3^{2-}, HCO_3^-, PO_4^{3-}, SO_4^{2-}, HSO_3^-, SCN^-, AcO^-, NO_3^-, NO_2^-, ClO_4^-, ClO_3^-, ClO_2^-, I^-, O_2^-, ROO• and H_2O_2) induced no detectable color and spectral changes. As displayed in **Fig. 1b**, when treated with CN^-, the fluorescence intensity at 450 nm of **2TM** was drastically enhanced upon an excitation at 350 nm, in accompaniment with a prominent fluorescence color change into bright blue under 365 nm irradiation, however, other tested anions and ROS exhibited no distinguished change. These changes indicate that **2TM** was only responsive to CN^- in aqueous media with high selectivity.

Fig. 1

Both excellent selectivity and anti-interference capability are two key parameters for evaluating the suitability of a developed sensor for biological and environmental applications. Thus, the specific selectivity of **2TM** in DMSO/H_2O (1:3, V/V) solution for CN^- was examined by introducing the related co-exist anions including Br^-, F^-, Cl^-, CO_3^{2-}, HCO_3^-, PO_4^{3-}, SO_4^{2-}, HSO_3^-, SCN^-, AcO^-, NO_3^-, NO_2^-, ClO_4^- and I^-. As shown in **Fig. S5**, in the presence of 10.0 equiv. CN^- and 10.0 equiv. other interfering co-existed anions, the changes of fluorescence intensity at 450 nm were similar to that induced by only CN^-, indicating that sensor **2TM** towards CN^- in aqueous media showed excellent selectivity and anti-interference capability.

To further investigate the interaction between **2TM** and CN^-, the optical titrations of CN^- (0–2 equiv.) were carried out in DMSO/H_2O (1:3, V/V) solution. With successive addition of CN^- to **2TM** solution, the absorption peak at 452 nm decreased progressively with the simultaneous occurrence of a new peak at 315 nm, indicating that the intramolecular charge transfer (ICT) transition within the sensor **2TM** molecule from the electron-rich bithiophene unit to the electron-deficient Meldrum's acid unit is blocked [58,59]. Meanwhile, an isosbestic point appeared at 360 nm,

implying a new species was generated during the UV-Vis titration process (**Fig. 2a**). On the other hand, with the addition of increasing CN^-, the sensor **2TM** displayed a turn-on fluorescence emission, the fluorescence intensity at 450 nm increased gradually and reached saturation when 1.0 equiv. CN^- was added (**Fig. 2b**). These great spectral changes can be explained by that the nucleophilic attack of CN^- to **2TM** destroyed the π-conjugated system. A good linear relationship between fluorescence intensity at 450 nm and CN^- concentration at a range of 0–10 μM with a correlation coefficient R^2 = 0.99857 was obtained (**Fig. S6**), indicating the 1:1 nucleophilic addition reaction between **2TM** and CN^-. In addition, the 1:1 stoichiometry interaction between **2TM** and CN^- was also confirmed by Job's plot analysis [60] (**Fig. S7**). The detection limit (DL) of sensor **2TM** for CN^- was estimated to be 0.96 μM based on 3σ/k [61,62], which is much lower than the maximum level of WHO (1.9 μM) in drinking water, implying **2TM** was an effective tool to quantitatively and sensitively detect trace CN^- in real water samples.

Fig. 2

Rapid response of a developed sensor towards a special analyte is an important factor to evaluate its real-time detection performance in practical applications, hence, the time-dependent experiment of **2TM** towards CN^- was executed in DMSO/H_2O (1:3, V/V) solution. As illustrated in **Fig. 3a**, the change of the fluorescence intensity at 450 nm is completed within 30 s with addition of CN^- and keeps on a steady value as prolonged reaction time, indicating that the **2TM** could be useful for rapid and real-time detection of CN^- in aqueous media. In addition, the pH effect on real-time detection is another key parameter in real samples, therefore, the pH effects on the fluorescence response of **2TM** (10 μM) in the absence and presence of CN^- (2.0 equiv.) were also measured in DMSO/H_2O (1:3, V/V) solution. As illustrated in **Fig. 3b**, in the absence of CN^-, no obvious change in fluorescence intensity at 450 nm of **2TM** was observed over the pH range 5-11. However, in the presence of CN^-, the fluorescence intensity at 450 nm of **2TM** showed a significant fluorescence enhancement and were maintained over a wide pH range 5-10, but the fluorescence intensity decreased below pH 5 owing to the protonation of cyanide anions. Therefore, the **2TM** showed highly sensitive fluorescent sensor for CN^- in the wide pH range 5-10 and could be used to conveniently and effectively detect CN^- in both environmental and physiological conditions.

Fig. 3

*3.2 Spectroscopic response of **2TM** towards ClO^-*

The UV–vis absorption and fluorescence responses of **2TM** in the presence of various anions and ROS including ClO^-, Br^-, F^-, Cl^-, CO_3^{2-}, HCO_3^-, PO_4^{3-}, SO_4^{2-}, HSO_3^-, SCN^-, AcO^-, NO_3^-, NO_2^-, ClO_4^-, ClO_3^-, ClO_2^-, I^-, O_2^-, H_2O_2 and ROO• were investigated in ～100% aqueous solution. As depicted in **Fig. 4a**, after addition of 2.0 equiv. ClO^- to **2TM** (10 μM) solution, the strong absorption band at 452 nm disappeared and a new absorption band emerged at 362 nm, along with a dramatic solution color change from yellow to colorless, whereas no significant spectral and solution color changes were noticed in the presence of other tested anions. As displayed in **Fig. 4b**, the fluorescence intensity at 452 nm of **2TM** in ～100% aqueous solution was greatly enhanced accompanied with a distinct fluorescence color change from dark blue to bright blue by naked eyes in the presence of 2.0 equiv. ClO^-, while no color and spectral changes were detected in the presence of other tested analytes. These investigations indicate that **2TM** can selectively sense ClO^- in ～100% aqueous solution. Subsequently, the specific selectivity of **2TM** for ClO^- was evaluated by adding 10.0 equiv. of different analytes in ～100% aqueous solution (**Fig. S8**). The treatment of other analytes each caused no significant fluorescence

changes in the sensor **2TM**. We further added different analytes to **2TM**, and then added 10.0 equiv. ClO^- to verify the anti-interference ability of **2TM**. The results demonstrated that sensor **2TM** showed high specific selectivity and excellent anti-interference for ClO^- detection.

Fig. 4

The spectroscopic experiment was executed to understand the interaction between **2TM** and ClO^- in ～100% aqueous solution. As shown in **Fig. 5a**, upon incremental addition of ClO^- (0–20 μM), the absorption band at 452 nm was gradually decreased up to disappear and a new absorption peak at 362 nm was steadily increased, a clear isosbestic point at 392 nm was easily observed, indicating a new species was formed during the titration process. Meanwhile, the changes in the fluorescence spectra of **2TM** (10 μM) upon addition of ClO^- (0–2 equiv.) in ～100% aqueous solution was exhibited in **Fig. 5b**. The fluorescence intensity at 452 nm increased gradually by the incremental addition of ClO^- with a saturation observed at 10 μM ClO^-. A good linear relationship between fluorescence intensity at 452 nm and ClO^- concentration (0−10 μM) with a good correlation coefficient R^2 = 0.99808 was derived (**Fig. S9**), suggesting that

the quantification of ClO^- in ～100% aqueous solution by **2TM** was feasible. A fitting of this titration data indicates 1:1 ratio interaction between the **2TM** and ClO^-, and this 1:1 stoichiometry was further verified by Job's plot (**Fig. S10**). The detection limit of **2TM** towards ClO^- was calculated to be 48.3 nM based on 3σ/k, which was superior to some reported ClO^--sensitive fluorescent sensors [63-65]. These results established that **2TM** could achieve sensitive and quantitative detection of ClO^- in ～100% aqueous media.

Fig. 5

Response time is of great importance for a sensor to validate its performance. Consequently, the time-dependent variation in fluorescence intensity at 450 nm for **2TM** in response to ClO^- in ～100% aqueous solution is evaluated (**Fig. 6a**). Upon the addition of 2.0 equiv. ～ClO^-, the fluorescence intensity at 452 nm of **2TM** dramatically enhanced and reached a plateau within 12 s, indicating that the reaction between **2TM** and ClO^- was nearly completed within 12 s. Such a quick response endowed the developed sensor **2TM** a promising potential for real-time monitoring of ClO^- in real samples. Next, the fluorescence response of **2TM** to ClO^- in

different pH values was conducted in ～100% aqueous media. As observed in **Fig. 6b**, the fluorescence intensity at 452 nm of free **2TM** was pH insensitive over a wide pH range 1–14. When 20 μM ClO^- was added, the fluorescence intensity at 452 nm increased and kept almost unchanged in a pH range 2–7. Therefore, **2TM** could be used for the real-time and sensitive detection of ClO^- in environmental and biological samples.

Fig. 6

3.3 Sensing mechanisms

To verify the sensing mechanism of **2TM** towards CN^-, ^1H NMR, FTIR, and HRMS spectra were measured before and after adding CN^- to **2TM**. As depicted in **Fig. 7a**, with addition of 1.0 equiv. CN^-, the vinyl proton H_a at 8.64 ppm disappeared and a new proton H_b at 5.26 ppm appeared, indicating the addition process of CN^- to vinyl group of **2TM**. Meanwhile, owing to breaking the conjugation via the CN^- nucleophilic addition, all the aromatic protons in **2TM** were obviously upfield shifted. In the FTIR spectra (**Fig. S11**), upon the addition of CN^-, the ester (O-C=O) group at 1717 cm^{-1} of **2TM** was shifted to 1620 cm^{-1}, meanwhile, the appearance of a new stretching vibration peak at 2143 cm^{-1} corresponds to the nitrile (C≡N) group, suggesting the CN^- addition to vinyl group in **2TM**. In the HRMS

spectrum, a new peak appeared at m/z = 351.0236 was attributed to the **3TBN-CN** adduct [**2TM** + CN + 4H]$^{4+}$ (351.0208), which revealed that the nucleophilic reaction between **2TM** and CN^- was proceeded in a molar ratio of 1:1 (**Fig. S12**). Together with the optical instruments, the plausible nucleophilic addition reaction between **2TM** and CN^- was well proposed and shown in **Scheme 2**. The nucleophilic attack of CN^- toward **2TM** interrupted the well π-conjugated system and effectively inhibited the ICT process, thus caused a significant fluorescence turn on response [66,67].

Next, the possible reaction between **2TM** and ClO^- was carefully analyzed by ^{1}H NMR, FTIR and HRMS spectra. After the reaction between **2TM** and ClO^-, there was a new proton peak appeared at about 9.80 ppm, which was attributed to the aldehyde proton (H_b) of the oxidative cleavage product **2T-CHO** (**Fig. 7b**), well matched with the ^{1}H NMR analysis of free compound **2T-CHO**. In the FTIR spectra (**Fig. S13**), after treatment of ClO^-, the ester (O-C=O) group at 1717 cm^{-1} of **2TM** disappeared, and a new stretching vibration peak at 1655 cm^{-1} was observed corresponding to the aldehyde (HC=O) group. Moreover, in the HRMS spectra (**Fig. S14**), the peak at m/z = 194.9926 was assigned to the oxidative cleavage product of **2T-CHO** [**2T-CHO** + H]$^+$ (194.9860). In addition, the significant optical spectral changes of **2TM** after treatment of excess ClO^- were well matched with that of free compound **2T-CHO** (**Fig. S15**). The aforementioned

evidences demonstrated that the reaction between **2TM** and ClO^- in ~ 100% aqueous solution was the ClO^--promoted oxidative cleavage of olefinic C=C bond to release the free fluorophore **2T-CHO** [68-70], led to prominent color and spectral changes (**Scheme 2)**.

Fig. 7

Scheme 2

3.4 Practical applications

To explore the practical utility of **2TM** for qualitative analysis of CN^- in real life, the food samples including the sprouted potato, cassava, immature sorghum and bitter seed were chosen for the experiments. The the sprouted potato, cassava, immature sorghum and bitter seed were separately smashed and soaked in 100 mL water for 3 days until the extract became turbid. The mixture was then filtered and washed three times with NaOH (100 mL, 100 mmol/L) to give a cyanide-containing solution and remained the solution pH < 8. As displayed in **Fig. 8**, when the four different cyanide solutions were added to **2TM** (10 μM), it's well worth noting that the fluorescence intensity increased significantly and the color changed to bright blue could be distinguished by the naked eyes under 365 nm UV light. These

investigated results showed that the recognition process is simple, handy, and fast response, thus, the **2TM** can be effectively utilized for real-time detection of CN^- in the natural food samples.

Fig. 8

To further exploit the practical application of **2TM** for quantitative analysis of CN^- and ClO^- in real water, we selected the distilled water, river water, tap water, the Yellow River water, lake water of Ji'nan Garden Expo as water samples for the experiment. The detection accuracy and relative standard deviation (RSD) was calculated by adding known concentrations of standard CN^- and ClO^- (1, 5 and 10 μM) to these samples. As displayed in **Tables 1** and **2**, the values of recovery were determined from 98% to 103% of **2TM** to CN^-, and from 98.6% to 102.1% of **2TM** to ClO^-, together with the obtained RSD values down to < 3.5%. The good recovery and excellent analytical precision showed that sensor **2TM** is feasible, accurate and reliable in the determination of CN^- and ClO^- in environmental samples.

Table 1

Table 2

Based on the excellent characteristics of the sensor **2TM**, we applied **2TM** to HeLa intracellular imaging to detect exogenous CN^- and ClO^-. The MTT assay showed that **2TD** has little cytotoxicity and was capable of bio-imaging application (**Fig. S16**). After the HeLa cells were incubated with **2TM** (15 μM) for 60 min, almost no fluorescence was exhibited under the blue channel (**Fig. 9a,b**). When the HeLa cells were incubated with 20 μM CN^-/ClO^- for 30 min, respectively, an obvious blue fluorescence signal occurred under blue channel (**Fig. 9c,d**). All the results illustrated that sensor **2TM** has good cell-membrane permeability and was capable of imaging intracellular CN^- and ClO^- in live cells.

Fig. 9

3.5 Detection on test strips

The development of colorimetric test strips for fast and convenient detection of CN^- and ClO^- could be important and useful for environmental samples. To verify the possibility of **2TM** as a fast and convenient economical portable tool for colorimetric and instant detection of CN^- and ClO^- in environmental water, the easy-to-use inexpensive test strips were fabricated by soaking filter papers/TLC plates in **2TM** solution (1 mM,

DMSO) and air-drying. As shown in **Fig. 10a**, the yellow-colored TLC plates were dipped in CN^-/ClO^- solutions (1 mM, water) showed immediately naked-eye discernible color change to colorless under daylight as well as an obvious fluorescence color change from green to blue. Further, the **2TM**-coated filter papers were immersed in CN^-/ClO^- solutions of different concentrations and dried in air. According to the increasing concentration of CN^-/ClO^-, the color was changed gradually from yellow to gray were clearly viewed under daylight, along with the fluorescence color changes from green to blue under 365 nm illumination (**Fig. 10b**). These observations implied that the test strips served as a practical tool to colorimetrically and conveniently monitor CN^- and ClO^- in water.

In addition, the silica loaded **2TM** was prepared and used for the selective detection of CN^-/ClO^-. The silica gels (100 mesh, 1 g) were loaded with **2TM** solution (1.0 mM) and dried under vacuum to obtain the yellow color. The dried silica was then added to CN^-/ClO^- (1.0 mM, water), the color immediately changed to colorless and blue under sunlight and UV light, respectively (**Fig. 10c**), which insisted on the real application of **2TM** for rapid and qualitative identification of CN^- and ClO^-. These results demonstrated that sensor **2TM** could selectively and visually recognize CN^- and ClO^- in water as a portable device by the naked eyes.

Interestingly, due to the above good fluorescent sensing performance, sensor **2TM** could serve as a rewritable small-molecular smart fluorescent display material. The CN^-/ClO^- solution (10 μM, water) was loaded into a pen without any modification and was used to write a letter of "CN^-, ClO^- and QLU", number of "2019" and Chinese characters (such as "Qilu University of Technology") on the **2TM**-based filter papers, respectively, and the results were visualized under 365 nm UV light. As displayed in **Fig. 10 (d)**, all the letter, number, and the Chinese characters on the handwritten filter paper gave bright blue fluorescence, further confirming **2TM** could be used as a convenient and inexpensive test tool for sensing CN^- and ClO^- in water.

Fig. 10

4. Conclusions

In summary, a novel dual-function bithiophene-Meldrum's acid based colorimetric and fluorescent sensor **2TM** was synthesized and characterized. On account of the outstanding advantages of excellent selectivity, great sensitivity, ultrafast response time and wide working pH range, sensor **2TM** was successfully applied to detecting CN^- and ClO^- in aqueous media with

naked-eye colorimetric and fluorescent turn-on responses, and its practical utility as an on-site testing reagent has been verified in live cells and environmental water samples. Moreover, the sensor **2TM** was also capable of monitoring CN^- in the natural food samples. In addition, colorimetric test strips demonstrated a promising application of **2TM** as a portable, eco-friendly and ultrafast device for real-time and on-site visual detection of CN^- and ClO^- in water with great sensitivity.

Acknowledgments

The authors gratefully acknowledge the financial support from the National Natural Science Foundation of China (Nos. 21776143, 21376125, 51702178 and 21801144), the Natural Science Foundation of Shandong Province (No. ZR2017LB009), the Program for College Students' Innovation and Entrepreneurship Training of Shandong Province (No. S201910431035), the Youth Innovative Talents Recruitment and Cultivation Program of Shandong Higher Education, and the Program for Scientific Research and the Program for Scientific Research Innovation Team in Colleges and Universities of Shandong Province (No. 0308150302).

References

[1] Baskin, S.I.; Brewer, T.G. Cyanide poisoning. In Medical Aspects of Chemical and Biological Warfare; F. Sidell, E.T. Takafuji, D.R. Franz, *Eds. TMM Publication Washington* **1997**, 271-268

[2] Kulig, K.W.U.S. Department of Health and Human Services. Cyanide Toxicity. *Atlanta* **1991**.

[3] Liu, S.Z; Yang, M.; Liu, Y.J.; Chen, H.B.; Li, H.M. A novel “turn-on” fluorescent probe based on triphenylimidazole-hemicyanine dyad for colorimetric detection of CN^- in 100% aqueous solution. *J. Hazard. Mater.* **2018**, 344, 875-882.

[4] Li, X.H.; Gao, X.H.; Shi, W.; Ma, H.M. Design strategies for water-soluble small molecular chromogenic and fluorogenic probes. *Chem. Rev.* **2014**, 114, 590-659.

[3] Kulig, K.W. Cyanide Toxicity, U.S. Department of Health and Human Services. *Atlanta* **1991**.

[4] Young, C.; Tidwell, L.; Anderson, C. Cyanide: Social, Industrial, and Economic Aspects. Minerals, Metals, and Materials Society. *Warrendale* **2001**, 34, 133-133.

[5] Wang, F.; Wang, L.; Chen, X.Q.; Yoon, J.Y. Recent progress in the development of fluorometric and colorimetric chemosensors for detection of cyanide ions. *Chem. Soc. Rev.* **2014**, 43, 4312-4324.

[6] Xu, Z.C.; Chen, X.Q.; Kim, H.N.; Yoon, J.Y. Sensors for the optical detection of cyanide ion, *Chem. Soc. Rev.* **2010**, 39, 127-137.

[7] Chen, Y.; Deterding, L.J.; Tomer, K.B.; Mason, R.P. Nature of the inhibition of horseradish peroxidase and mitochondrial cytochrome c oxidase by cyanyl radical. *Biochemistry* **2000**, 39, 4415-4422.

[8] Correia, S.C.; Santos, R.X.; Cardoso, S.M.; Santos, M.S.; Oliveira, C.R.; Moreira, P.I. Cyanide preconditioning protects brain endothelial and NT2 neuron-like cells against glucotoxicity: role of mitochondrial reactive oxygen species and HIF-1α. *Neurobiol. Dis.* **2012**, 45, 206-218.

[9] World Health Organization, Guidelines for Drinking-Water Quality. **1996**.

[10] Koide, Y.; Urano, Y.; Kenmoku, S.; Kojima, H.; Nagano, T. Design and synthesis of fluorescent probes for selective detection of highly reactive oxygen species in mitochondria of living cells. *J. Am. Chem. Soc.* **2007**, 129, 10324-10325.

[11] Chen, X.; Tian, X.; Shin, I.; Yoon, J. ChemInform abstract: fluorescent and luminescent probes for detection of reactive oxygen and nitrogen species. *Chem. Soc. Rev.* **2011**, 40, 4783-4804.

[12] Koide, Y.; Urano, Y.; Hanaoka, K.; Terai, T.; Nagano, T. Development of an Si-rhodamine-based far-red to near-infrared fluorescence probe

selective for hypochlorous acid and its applications for biological imaging. *J. Am. Chem. Soc.* **2011**, 133, 5680-5682.

[13] Best, Q.A.; Sattenapally, N.; Dyer, D.J.; Scott, C.N.; McCarroll, M.E. pH-Dependent si-fluorescein hypochlorous acid fluorescent probe: spirocycle ring-opening and excess hypochlorous acid-induced chlorination. *J. Am. Chem. Soc.* **2013**, 135, 13365-13370.

[14] Liu, Y.; Li, K.; Wu, M.Y.; Liu, Y.H.; Xie, Y.M.; Yu, X.Q. A mitochondria-targeted colorimetric and ratiometric fluorescent probe for biological SO2 derivatives in living cells. *Chem. Commun.* **2015**, 51, 10236-10239.

[15] Prokopowicz, Z.M.; Arce, F.; Biedron, R.; Chiang, C.L.L.; Ciszek, M.; Katz, D.R.; Nowakowska, M.; Zapotoczny, S.; Marcinkiewicz, J.; Chain, B.M. Hypochlorous acid: a natural adjuvant that facilitates antigen processing, cross-priming, and the induction of adaptive immunity. *J. Immunol.* **2010**, 184, 824-835.

[16] Rutala, W.A.; Weber, D.J. Uses of inorganic hypochlorite (bleach) in health-care facilities. *Clin. Microbiol. Rev.* **1997**, 10, 597-610.

[17] Guo, J.; Zhang, Z.X.; Kuai, Z.Y.; Wang, R.; Yang, Q.B.; Shan, Y.M.; Li, Y.X. A new turn-on fluorescent probe towards hypochlorite in living cells. *Anal. Methods.* **2017**, 9, 864-870.

[18] Shen, S.L.; Huang, X.Q.; Zhang, Y.Y.; Zhu, Y.; Hou, C.; Ge, Y.Q.; Cao, X.Q. Ratiometric fluorescent probe for the detection of HOCl in lysosomes based on FRET strategy. *Sens. Actuat. B Chem.* **2018**, 263, 252-257.

[19] Huang, Y.; Zhang, P.; Gao, M.; Zeng, F.; Qin, A.; Wu, S.; Tang, B. Z. Ratiometric detection and imaging of endogenous hypochlorite in live cells and in vivo achieved by using an aggregation induced emission (AIE)-based nanoprobe. *Chem. Commun.* **2016**, 52, 7288-7291.

[20] Li, D.W.; Sun, J.J.; Gan, Z.F.; Chen, H.Y.; Guo, D. Reaction-based SERS nanosensor for monitoring and imaging the endogenous hypochlorous acid in living cells. *Anal. Chim. Acta*. **2018**, 1018, 104-110.

[21] Fang, Q.; Tian, H.H.; Yang, L.; Chen, S.; Liu, X.J.; Song, X.Z. A thiocoumarin-based fluorescent probe for detection of hypochlorite with high selectivity over other typical desulfurizing agents (Hg^{2+}/Ag^{+}). *Sens. Actuat. B Chem.* **2018**, 260, 146-155.

[22] Marc, V.; Zhai, D.T.; Er, J.C.; Chang, Y.T. Combinatorial Strategies in Fluorescent Probe Development. *Chem. Rev.* **2012**, 112, 4391-4420.

[23] Guo, Z.; Niu, Q.; Li, T.; Highly sensitive oligothiophene-phenylamine-based dualfunctional fluorescence “turn-on” sensor for rapid and simultaneous detection of Al^{3+} and Fe^{3+}

in environment and food samples. *Spectrochim. Acta A* **2018**, 200, 76-84.

[24] Lan, L.; Niu, Q.; Li, T. A highly selective colorimetric and ratiometric fluorescent probe for instantaneous sensing of Hg^{2+} in water, soil and seafood and its application on test strips. *Anal. Chim. Acta* **2018**, 1023, 105-114.

[25] Niu, Q.; Wu, X.; Li, T.; Cui, Y.; Zhang, S.; Li, X. Highly selective, sensitive and fast-responsive fluorescent sensor for Hg^{2+}. *Spectrochim. Acta A* **2016**, 163, 45-48.

[26] Sun, T.; Niu, Q.; Guo, Z.; Li, T. A simple highly sensitive and selective turn-on fluorescent chemosensor for the recognition of Pb^{2+}. *Tetrahedron Lett.* **2017**, 58, 252-256.

[27] Li, Y.; Niu, Q.; Wei, T.; Li, T. Novel thiophene-based colorimetric and fluorescent turn-on sensor for highly sensitive and selective simultaneous detection of Al^{3+} and Zn^{2+} in water and food samples and its application in bioimaging. *Anal. Chim. Acta* **2019**, 1049, 196-212.

[28] Wang, J.; Wei, T.; Ma, F.; Li, T.; Niu, Q. A novel fluorescent and colorimetric dual-channel sensor for the fast, reversible and simultaneous detection of Fe^{3+} and Cu^{2+} based on terthiophene derivative with high sensitivity and selectivity. *J. Photoch. Photobio. A: Chem.* **2019**, 383, 111982.

[29] Guo, Z.; Hu, T.; Wang, X.; Sun, T.; Li, T.; Niu, Q. Highly sensitive and selective fluorescent sensor for visual detection of Cu^{2+} in water and food samples based on oligothiophene derivative. *J. Photoch. Photobio. A: Chem.* **2019**, 371, 50-58.

[30] Wang, J.; Niu, Q.; Hu, T.; Wei, T.; Li, T. A new phenothiazine-based sensor for highly selective, ultrafast, ratiometric fluorescence and colorimetric sensing of Hg^{2+}: Applications to bioimaging in living cells and test strips. *J. Photoch. Photobio. A: Chem.* **2019**, 384, 112036.

[31] Zuo, Z.; Song, X.; Guo, D.; Guo, Z.; Niu, Q. A dual responsive colorimetric/fluorescent turn-on sensor for highly selective, sensitive and fast detection of Fe^{3+} ions and its applications. *J. Photoch. Photobio. A: Chem.* **2019**, 382, 111876.

[32] Guo, Z.; Niu, Q.; Li, T.; Wang, E. Highly chemoselective colorimetric/fluorometric dual-channel sensor with fast response and good reversibility for the selective and sensitive detection of Cu^{2+}. *Tetrahedron* **2019**, 75, 3982-3992.

[33] Guo, Z.; Niu, Q.; Li, T.; Sun, T.; Chi, H. A fast, highly selective and sensitive colorimetric and fluorescent sensor for Cu^{2+} and its application in real water and food samples. *Spectrochim. Acta A* **2019**, 213, 97-103.

[34] Yin, P.; Niu, Q.; Yang, Q.; Lan, L.; Li, T. A new "naked-eye" colorimetric and ratiometric fluorescent sensor for imaging Hg^{2+} in living cells. *Tetrahedron* **2019**, 75, 130687.

[35] Yin, P.; Niu, Q.; Wei, T.; Li, T.; Li, Y.; Yang, Q. A new thiophene-based dual functional chemosensor for ultrasensitive colorimetric detection of Cu^{2+} in aqueous solution and highly selective fluorimetric detection of Al^{3+} in living cells. *J. Photoch. Photobio. A: Chem.* **2020**, 389, 112249.

[36] Li, C.; Niu, Q.; Wang, J.; Wei, T.; Li, T.; Chen, J.; Qin, X.; Yang, Q. Bithiophene-based fluorescent sensor for highly sensitive and ultrarapid detection of Hg^{2+} in water, seafood, urine and live cells. *Spectrochim. Acta A* **2020**, 233, 118208.

[37] Wu, X.; Niu, Q.; Li, T.; Cui, Y.; Zhang, S. A highly sensitive, selective and turn-off fluorescent sensor based on phenylamine-oligothiophene derivative for rapid detection of Hg^{2+}. *J. Lumin.* **2016**, 175, 182-186.

[38] Xu, Z.;. Chen, X; Kim, H.N.; Yoon, J. Sensors for the optical detection of cyanide ion. *Chem. Soc. Rev.* **2010**, 39, 127-137.

[39] Wang, F.; Wang, L.; Chen, X.; Yoon, J. Recent progress in the development of fluorometric and colorimetric chemosensors for detection of cyanide ions, *Chem. Soc. Rev.* **2014**, 43, 4312-4324.

[40] Santos-Figueroa, L.E.; Moragues, M.E.; Climent, E.; Agostini, A.; Martínez-Máñez, R.; Sancenón, F. Chromogenic and fluorogenic

chemosensors and reagents for anions. A comprehensive review of the years 2010-2011. *Chem. Soc. Rev.* **2013**, 42, 3489-3613.

[41] Jo, J.; Olasz, A.; Chen, C.H.; Lee, D. Interdigitated Hydrogen Bonds: Electrophile Activation for Covalent Capture and Fluorescence Turn-On Detection of Cyanide. *J. Am. Chem. Soc.* **2013**, 135, 3620-3632.

[42] Ren, M.; Deng, B.; Zhou, K.; Kong, X.; Wang, J.Y.; Xu, G.; Lin, W. A lysosome-targeted and ratiometric fluorescent probe for imaging exogenous and endogenous hypochlorous acid in living cells. *J. Mater. Chem. B* **2016**, 4, 4739-4745.

[43] Yang, Y.T.; Yin, C.X.; Huo, F.J.; Chao, J.B.; Zhang, Y.B.; Cheng, F.Q. A new highly selective and turn-on fluorescence probe for detection of cyanide. *Sens. Actuat. B Chem.* **2014**, 193, 220-224.

[44] Manjare, S.T.; Kim, J.; Lee, Y.; Churchill, D.G. Facile meso-BODIPY annulation and selective sensing of hypochlorite in water. *Org. Lett.* **2014**, 16 520-523.

[45] Niu, Q.; Lan, L.; Li, T.; Guo, Z.; Jiang, T.; Zhao, Z.; Feng, Z.; Xi, J. A highly selective turn-on fluorescent and naked-eye colorimetric sensor for cyanide detection in food samples and its application in imaging of living cells. *Sens. Actuat. B Chem.* **2018**, 276, 13-22.

[46] Sun, T.; Niu, Q.; Li, Y.; Li, T.; Hu, T.; Wang, E.; Liu, H. A novel oligothiophene-based colorimetric and fluorescent “turn on” sensor for highly selective and sensitive detection of cyanide in aqueous media and its practical applications in water and food samples. *Sens. Actuat. B Chem.* **2018**, 258, 64-71.

[47] Guo, Z.; Hu, T.; Sun, T.; Li, T.; Chi, H.; Niu, Q. A colorimetric and fluorometric oligothiophene-indenedione-based sensor for rapid and highly sensitive detection of cyanide in real samples and bioimaging in living cells. *Dyes Pigm.* **2019**, 163, 667-674.

[48] Guo, Z.; Niu, Q.; Yang, Q.; Li, T.; Chi, H. A highly selective and sensitive dual-mode sensor for colorimetric and turn-on fluorescent detection of cyanide in water, agro-products and living cells. *Anal. Chim. Acta* **2019**, 1065, 113–123.

[49] Lan, L.; Li, T.; Wei, T.; Pang, H.; Sun, T.; Wang, E.; Liu, H.; Niu, Q. Oligothiophene-based colorimetric and ratiometric fluorescence dual-channel cyanide chemosensor: Sensing ability, TD-DFT calculations and its application as an efficient solid state sensor. *Spectrochim. Acta A* **2018**,193, 289-296.

[50] Lv, J.; Chen, Y.; Wang, F.; Wei, T.; Zhang, Z.; Qiang, J.; Chen, X.; A mitochondriatargeted fluorescent probe based on fluorescein derivative

for detection of hypochlorite in living cells. *Dyes Pigm.* **2017**, 148, 353-358.

[51] Lv, J.; Wang, F.; Wei, T.W.; Chen, X.Q. Highly Sensitive and Selective Fluorescent Probes for the Detection of HOCl/OCl^- Based on Fluorescein Derivatives. *Ind. Eng. Chem. Res.* **2018**, 13, 3757-3764

[52] Chen, Y.H.; Wei, T.W.; Zhang, Z.J.; Zhang, W.; Lv, J.; Chen, T.T.; Chi, B.; Wang, F.; Chen, X.Q. A mitochondria-targeted fluorescent probe for ratiometric detection of hypochlorite in living cells. *Chinese Chem. Lett.* **2017**, 28, 1957-1960

[53] Pan, H.; Liu, Y.; Liu, S.; Ou, Z.; Chen, H.; Li, H. A dual-function colorimetric probe based on cyanine-carbazole dyad for highly sensitive recognition of cyanide and hypochlorite in aqueous media, *Talanta* **2019**, 202, 329-335

[54] Li, Q.; Nie, J.; Shan, Y.; Li, Y.; Du, J.; Zhu, L.; Yang, Q.; Bai, F. Water-soluble fluorescent probe for simultaneous detection of cyanide, hypochlorite and bisulfite at different emission wavelengths. *Anal. Biochem.* **2020**, 591, 113539- 113551

[55] Malkondu, S.; Erdemir, S.; Karakurt, S. Red and blue emitting fluorescent probe for cyanide and hypochlorite ions: Biological sensing and environmental analysis. *Dyes Pigm.* **2019**, 174, 108019.

[56] Niu, Q.; Lu, Y.; Sun, H.; Li, X.; Tao, X. Novel phenyl-oligothiophene derivatives containing acetylenic spacers for thin film materials: Synthesis, photophysical and morphology properties. *Dyes Pigm.* **2013**, 97, 184-197.

[57] Wu, C.G.; Chung, M.F.; Tsai, H.H.G.; Tan, C.J.; Chen, S.C.; Chang, C.H.; Shih, T.W. Fluorene-Containing Organic Photosensitizers for Dye-Sensitized Solar Cells. *ChemPlusChem* **2012**, 77, 832-843.

[58] Pati, P.B. Organic chemodosimeter for cyanide: A nucleophilic approach. *Sens. Actuat. B Chem.* **2016**, 222, 374-390.

[59] Lee, J.J.; Park, G.J.; Choi, Y.W.; You, G.R.; Kim, Y.S.; Lee, S.Y.; Kim, C. Detection of multiple analytes (CN^- and F^-) based on a simple pyrazine-derived chemosensor in aqueous solution: experimental and theoretical approaches. *Sens. Actuat. B Chem.* **2015**, 207, 123-132.

[60] Job, P. Formation and stability of inorganic complexes in solution. *Ann. Chim.* **1928**, 9, 113-203.

[61] Analytical Methods Committee, Recommendations for the definition, estimation and use of the detection limit. *Analyst* **1987**, 112, 199-204.

[62] Tsui, Y.; Devaraj, S.; Yen, Y. Azo dyes featuring with nitrobenzoxadiazole (NBD) unit: A new selective chromogenic and fluorogenic sensor for cyanide ion. *Sens. Actuat. B Chem.* **2012**, 161, 510-519.

[63] Zhao, X.J.; Jiang, Y.R.; Chen, Y.X.; Yang, B.Q.; Li, Y.T.; Liu, Z.H.; Liu, C. A new“off-on” NIR fluorescence probe for determination and bioimaging of mitochondrial hypochlorite in living cells and zebrafish. *Spectrochim. Acta Part A* **2019**, 219, 509-516.

[64] Tang, X.; Zhu, Z.; Liu, R.; et al. A novel ratiometric and colorimetric fluorescent probe for hypochlorite based on cyanobiphenyl and its applications. *Spectrochim. Acta Part A* **2019**, 219, 576-581.

[65] Wang, S.C.; Zhang, B.Y.; Wang, W.J.; Feng, G.; Yuan, D.Q.; Zhang, X.J. Elucidating the Structure-Reactivity Correlations of Phenothiazine based Fluorescent Probes toward ClO^-. *Chem. Eur. J.* **2018**, 24, 8157-8166.

[66] Hu, Y.Q.; Xu, Z.; Zhang, S.; Wu, X.; Ding, J.W.; Lv, Z.S.; Feng, L.S. Recent developments of coumarin-containing derivatives and their anti-tubercular activity. *Eur. J. Med. Chem.* **2017**, 136, 122-130.

[67] Wang, Y.; Wang, J.; Xian, Q. A highly selective fluorescent and chromogenic probe for CN^- detection and its applications in bioimaging. *Talanta* **2018**, 190, 487-91.

[68] Pan, H.; Liu, Y.; Liu, S.; Ou, Z.; Chen, H.; Li, H. A dual-function colorimetric probe based on Carbazole-Cyanine dyad for highly sensitive recognition of cyanide and hypochlorous acid in aqueous media. *Talanta* **2019**, 202, 329-35.

[69] Xiao, H.; Li, J.; Zhao, J.; Yin, G.; Quan, Y.; Wang, J.; Wang, R. A colorimetric and ratiometric fluorescent probe for ClO^- targeting in mitochondria and its application in vivo. *J. Mater. Chem. B* **2015**, 3, 1633-1638.

[70] Wang, H.; He, Y.; Li, Y.; Zhang, C.; Zhang, P.; Cui, J.; Long, Y.; Chen, S.; Zeng, R.; Chen, J. Selective ratiometric fluorescence detection of hypochlorite by using aggregation-induced emission dots. *Anal. Bioanal. Chem.* **2019**, 411, 1979-88.

Figure and Table captions

Scheme 1. The synthetic route of sensor **2TM**.

Fig. 1 Absorption **(a)** and emission **(b)** spectra of sensor **2TM** (10 μM) in DMSO/H_2O (1/3, v/v) solution in the presence of CN^- and other analytes (2.0 equiv.); **Insets**: Visual solution color changes in **2TM** treated with various analytes.

Fig. 2 Absorption **(a)** and emission **(b)** spectra of **2TM** (10 μM) in DMSO/H_2O (1/3, v/v) treated with different concentrations of CN^- (0–2.0 equiv.).

Fig. 3 (a) Time-dependent **(a)** and pH effect **(b)** on the fluorescence intensity of **2TM** (10 μM) in DMSO/H_2O (1:3, v/v) in the absence or presence of 2.0 equiv CN^-.

Fig. 4 Absorption **(a)** and emission **(b)** spectra of sensor **2TM** (10 μM) in 100% aqueous solution in the presence of ClO^- and other analytes (2.0 equiv.); **Insets**: Visual solution color changes in **2TM** treated with various analytes.

Fig. 5(a) Absorption **(a)** and emission **(b)** spectra of **2TM** (10 μM) in 100% aqueous solution treated with various concentration of ClO^- (0–2.0 equiv.).

Fig. 6 Time-dependent **(a)** and pH effect **(b)** on the fluorescence intensity of **2TM** (10 μM) in 100% aqueous solution in the absence or presence of 2.0 equiv ClO^-.

Fig. 7. ^{1}H NMR spectra of **2TM** in the absence and presence of 1.0 equiv. **(a)** CN^-/ClO^- and **2T-CHO (b)** in DMSO-d_6.

Scheme 2. The proposed sensing mechanism of **2TM** and CN^-/ClO^- with observed colorimetric changes.

Fig. 8. Fluorescence spectral response of **2TM** (10 μM) in the sprouted potato, cassava, immature sorghum and bitter seed. **Insets**: the photograph of the sprouted potato, cassava, immature sorghum and bitter seed, and after addition of cyanide-containing, the color change of **2TM** under 365 nm UV light.

Fig. 9. Fluorescence images of HeLa cells incubated with **2TM** (15 μM) for 60 min **(a, b)**; Fluorescence images of **2TM**-loaded cells were further cultured with 20 μM of CN^- **(c)** and ClO^- **(d)** for 30 min, respectively.

Fig. 10(a) Photographs of TLC-based test strips of **2TM**, **2TM**+CN^-, and **2TM**+ClO^- by naked eyes; **(b)** Photographs of **2TD** treated with increasing CN^-/ClO^- concentration on filter papers; **(c)** Color changes of **2TM** in the solid state upon treatment of CN^-/ClO^- aion; **(d)** The photographic images of the fluorescent letter/text written on **2TM**-loaded filter paper using CN^- (left) and ClO^- (right) solution under UV light.

Table 1 Determination of CN^- in the environmental water samples.

Table 2 Determination of ClO^- in the environmental water samples.

Scheme 1

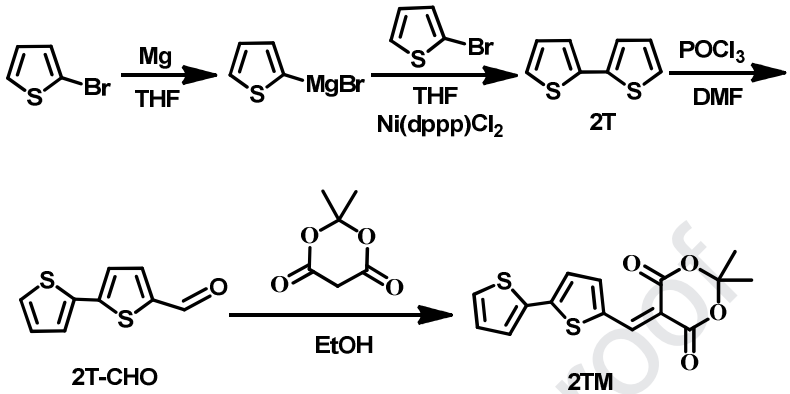

Fig. 1(a)

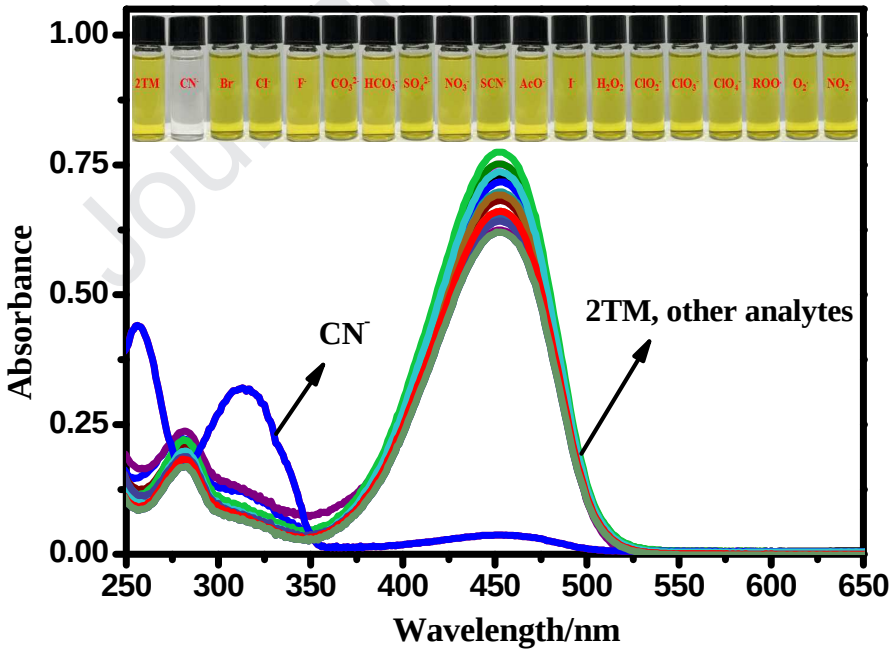

Fig. 1(b)

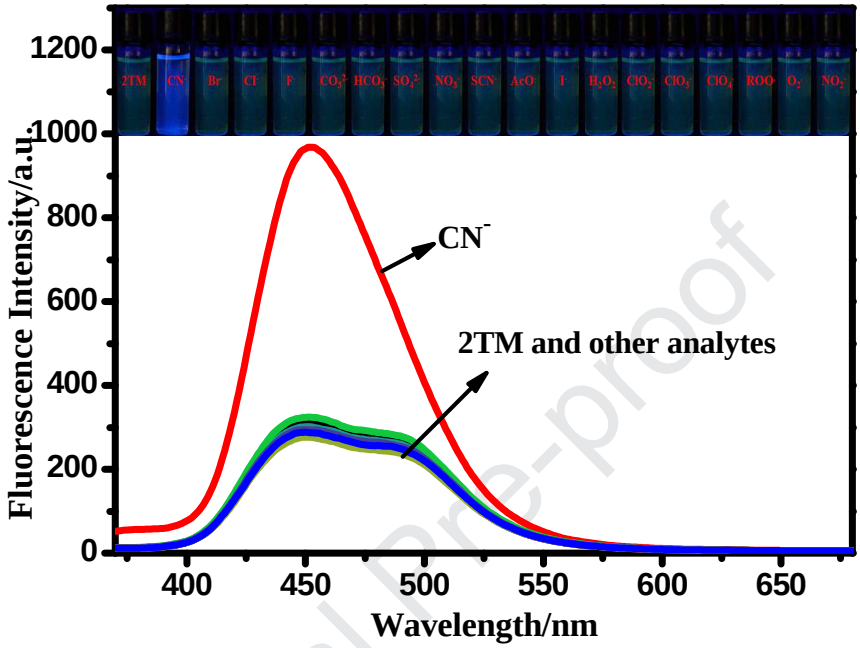

Fig. 2(a)

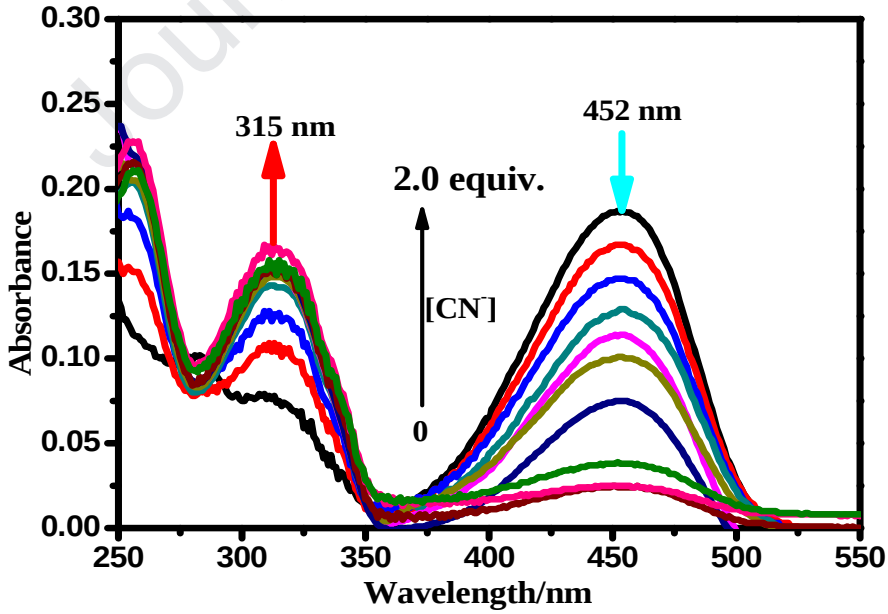

Fig. 2(b)

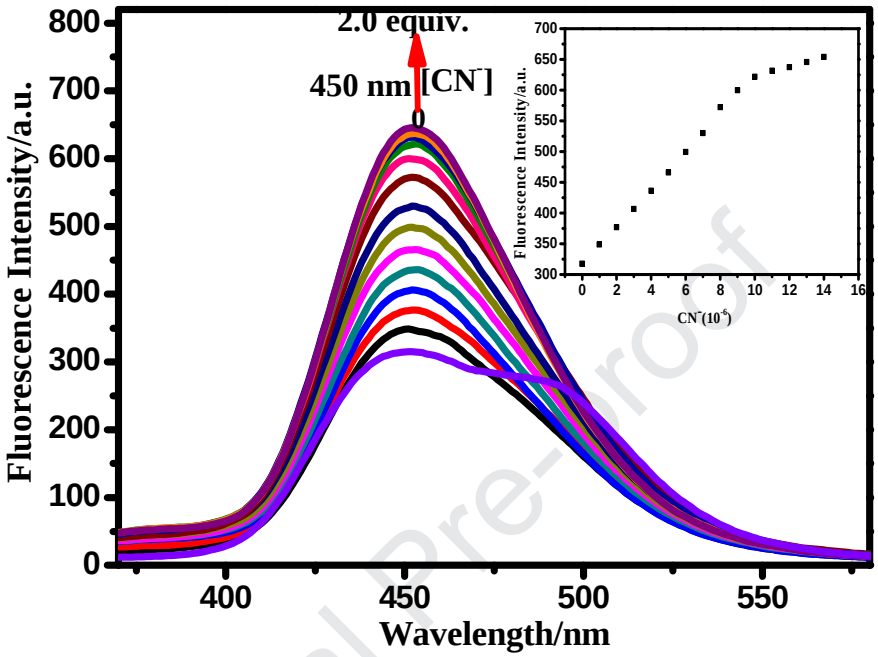

Fig. 3(a)

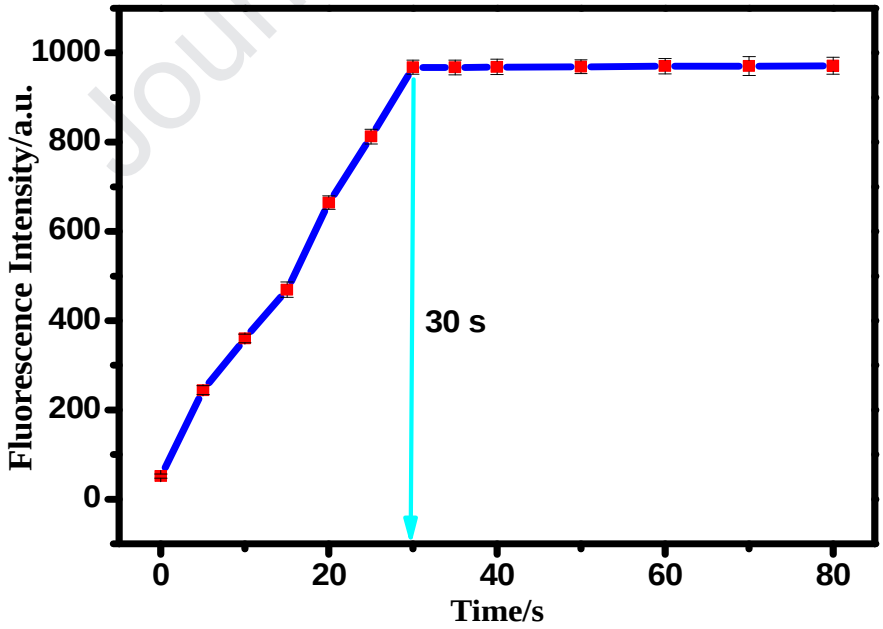

Fig. 3(b)

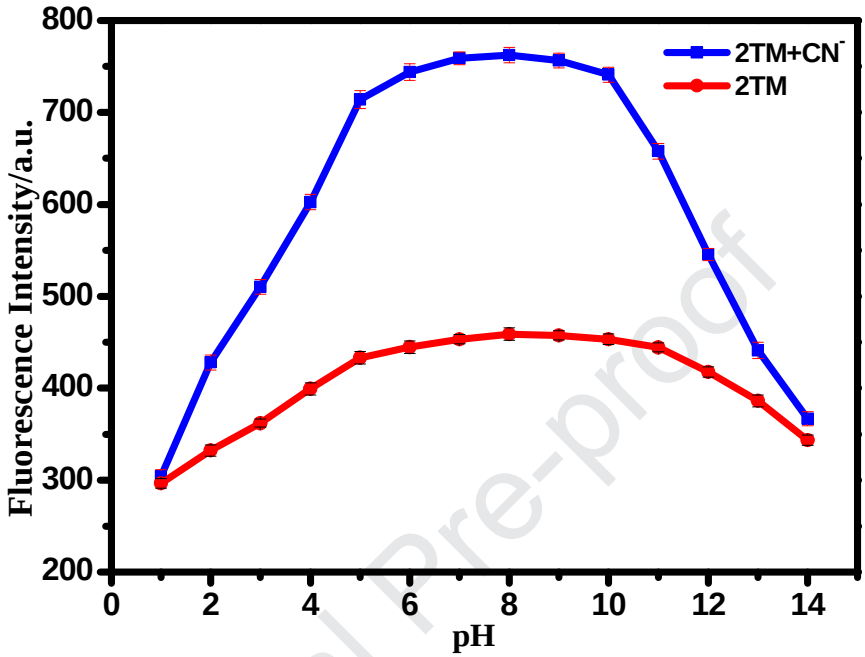

Fig. 4(a)

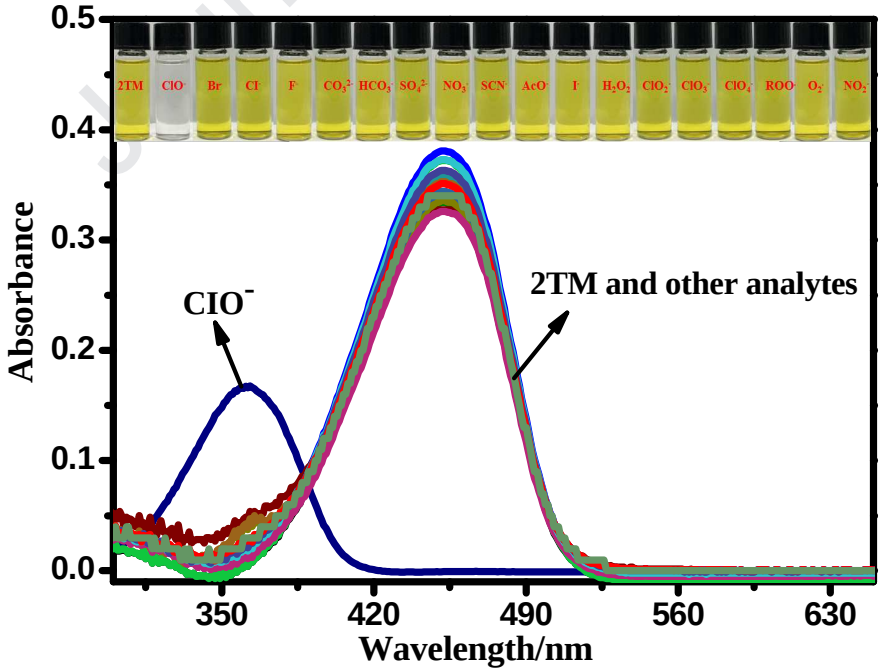

Fig. 4(b)

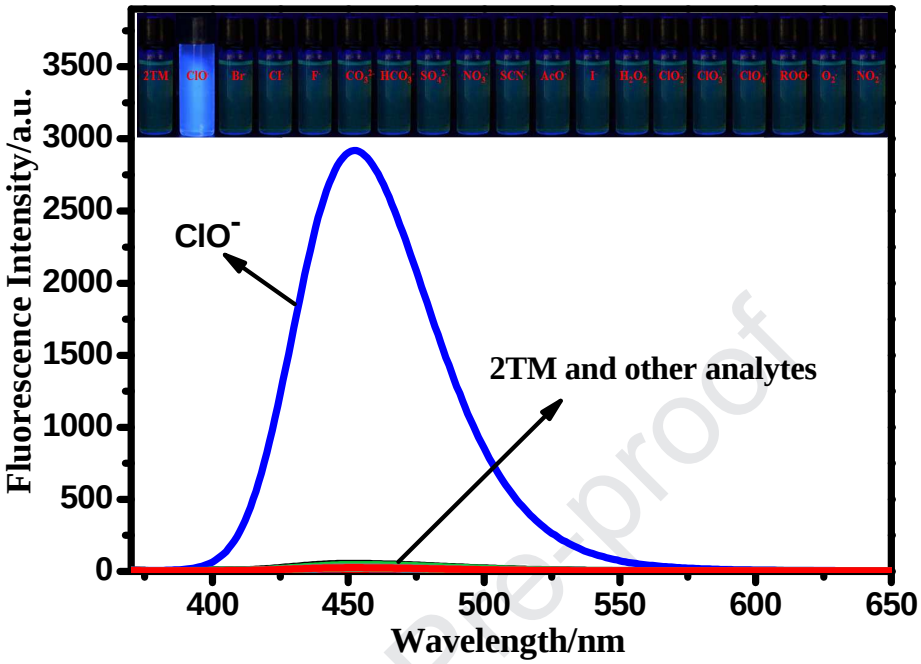

Fig. 5(a)

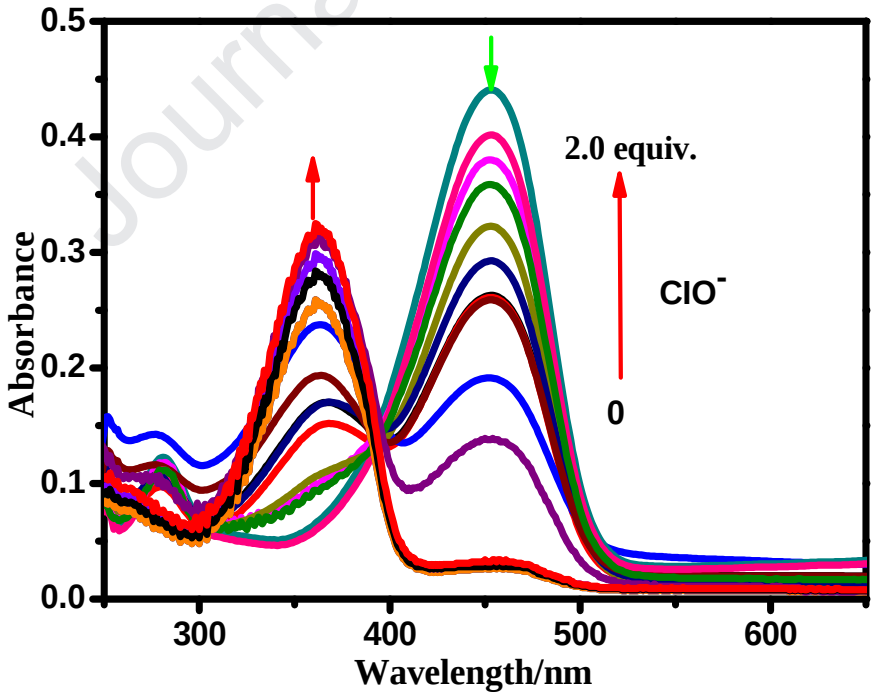

Fig. 5(b)

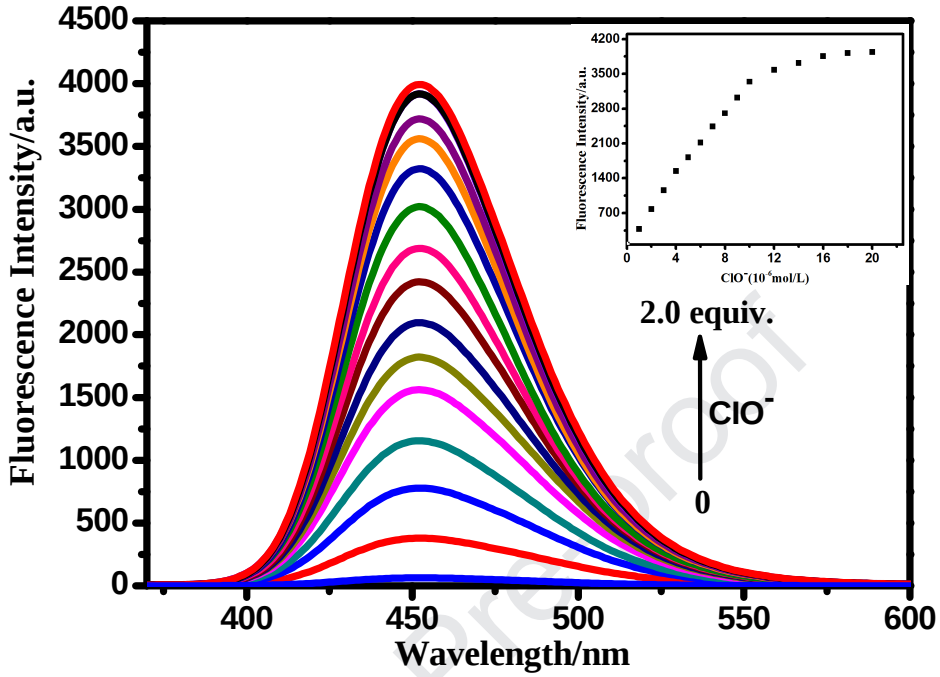

Fig. 6(a)

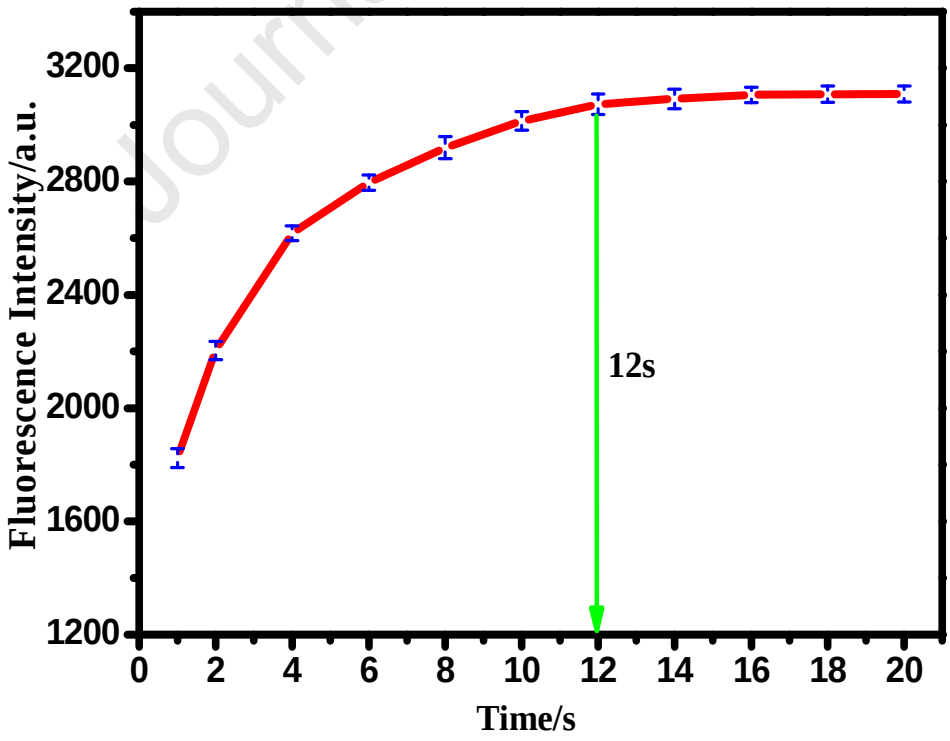

Fig. 6(b)

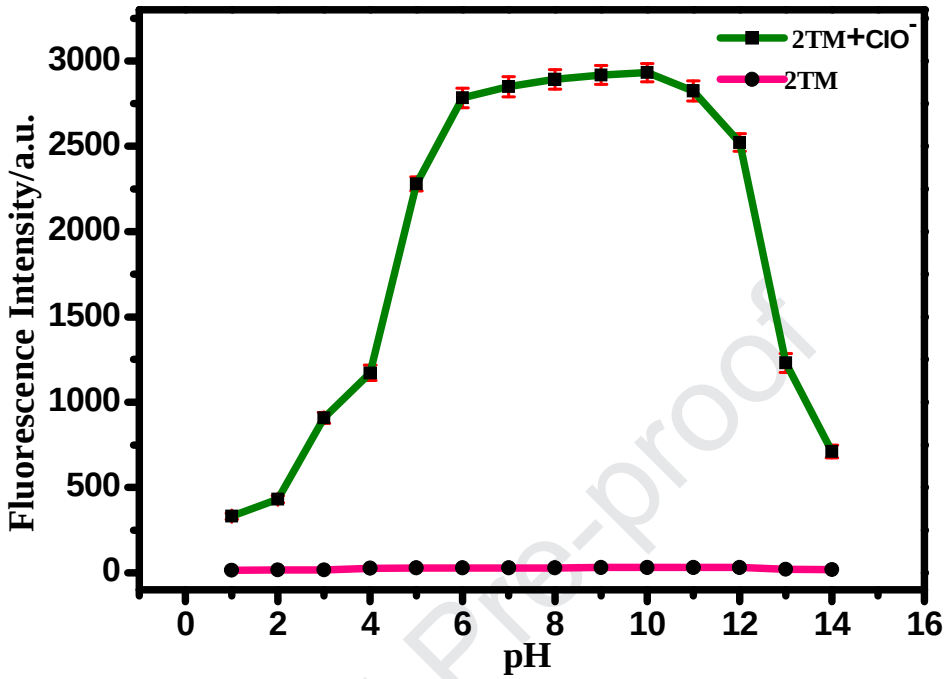

Fig. 7(a)

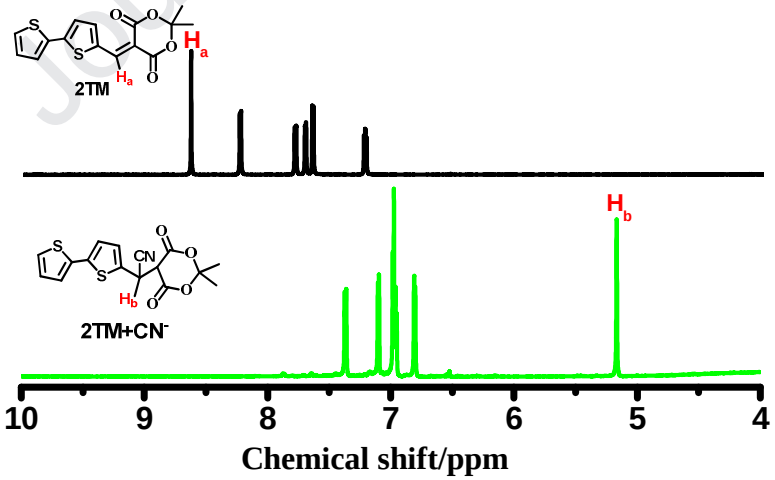

Fig. 7(b)

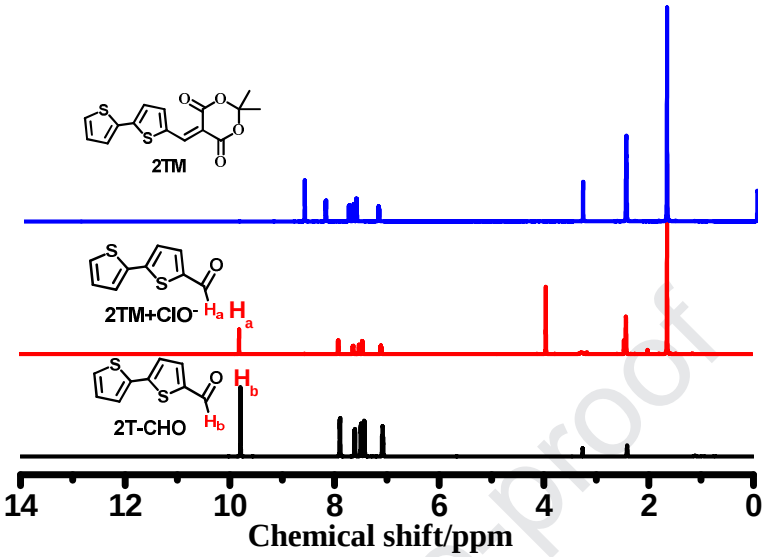

Scheme 2

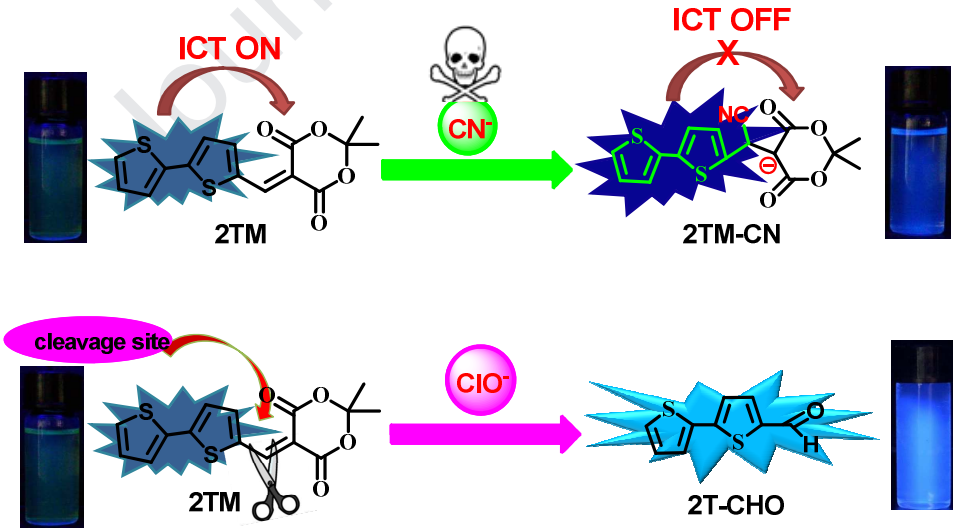

Fig. 8

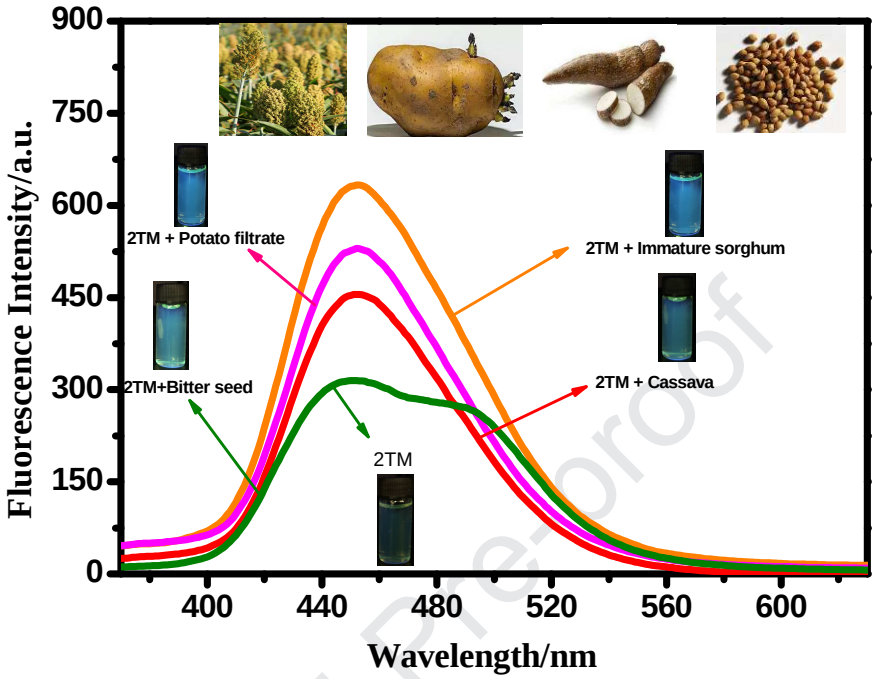

Fig. 9

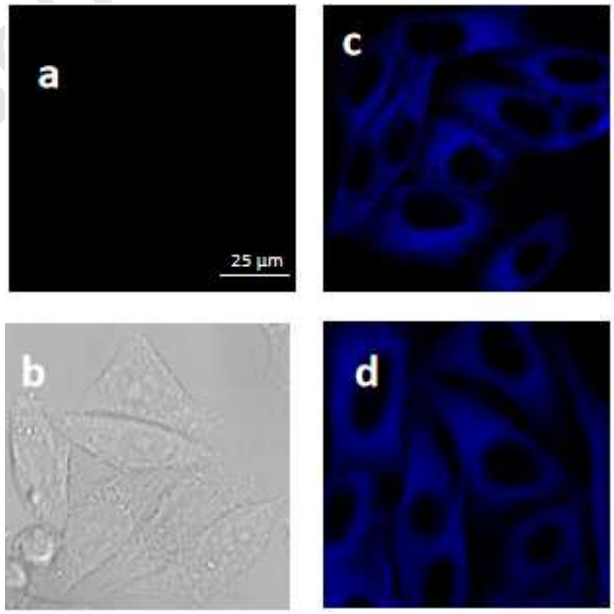

Fig. 10(a)

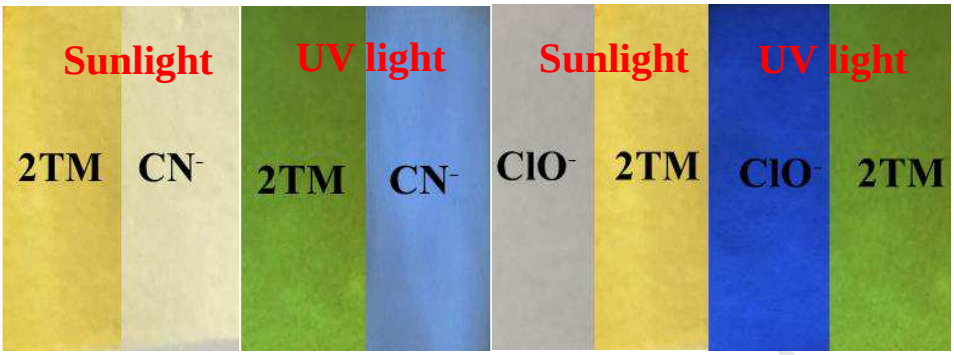

Fig. 10(b)

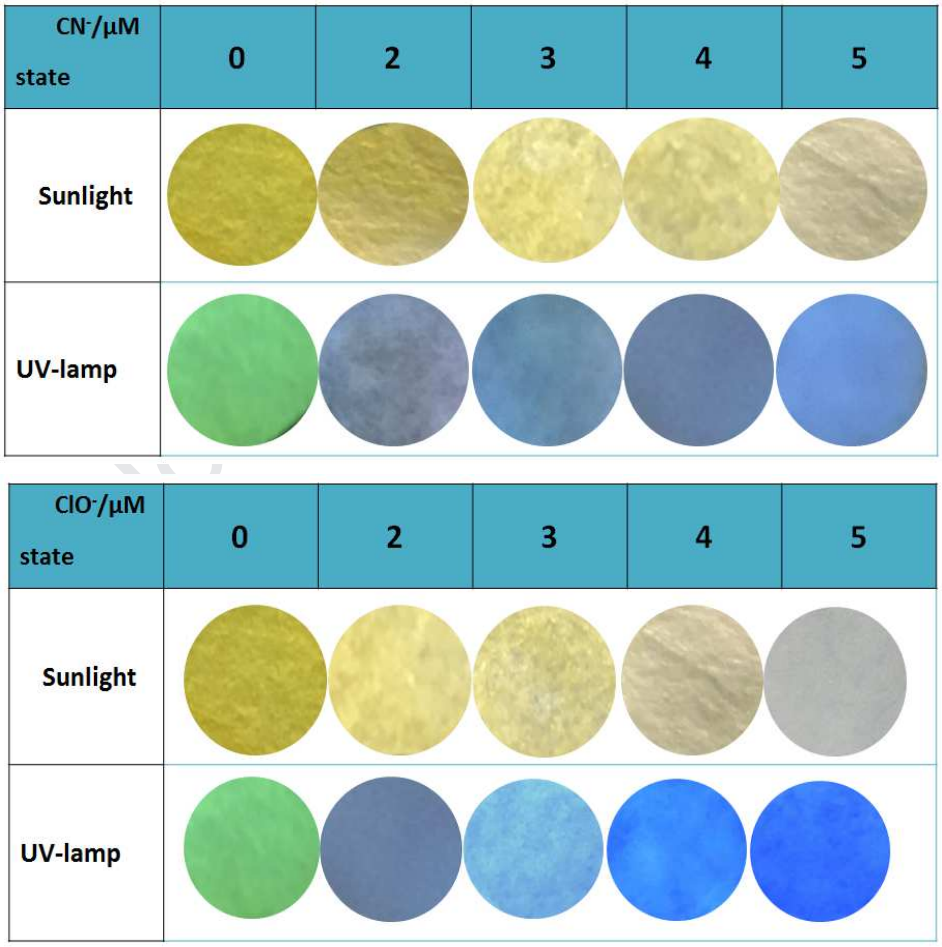

Fig. 10(c)

Fig. 10(d)

Table 1

Sample	Added（μM）	Detected（$\bar{x}$±SD）（μM）	Recovery（%）	RSD（n=5,%）
Distilled Wate	1	1.01±0.028	101%	2.7
	5	5.03±0.021	100.6%	0.42
	10	10.03±0.026	100.3%	0.26
River Water	1	1.02±0.026	102%	2.5
	5	4.99±0.032	99.8%	0.64
	10	9.99±0.011	99.9%	0.11
Tap Water	1	0.98±0.028	98%	2.8
	5	5.03±0.032	100.6%	0.64
	10	10.08±0.035	100.8%	0.35
Yellow River water	1	1.03±0.035	103%	3.3
	5	5.04±0.049	100.8%	0.98
	10	10.07±0.026	100.7%	0.26
Lake Water of Ji'nan Garden Expo	1	0.99±0.019	99.0%	1.9
	5	4.97±0.028	99.4%	0.56
	10	10.04±0.021	100.4%	0.21

Table 2

Sample	Added（μM）	Detected（$\bar{x}$±SD）（μM）	Recovery（%）	RSD（n=5,%）
Distilled Wate	1	1.03±0.025	101.8%	2.1
	5	5.07±0.019	101.4%	0.38
	10	10.03±0.023	100.3%	0.23
River Water	1	0.98±0.024	98.6%	2.3
	5	4.97±0.027	99.4%	0.54
	10	10.02±0.011	100.2%	0.11
Tap Water	1	1.05±0.023	102%	2.3
	5	5.09±0.028	101.8%	0.56
	10	10.07±0.035	100.7%	0.35
Yellow River water	1	1.03±0.035	102.1%	2.3
	5	4.99±0.049	99.8%	0.98
	10	10.03±0.022	100.3%	0.22
Lake Water of Ji'nan Garden Expo	1	1.01±0.023	101%	2.3
	5	4.98±0.031	99.6%	0.62
	10	10.02±0.028	100.2%	0.28

Highlights

►A novel colorimetric and fluorescent sensor **2TM** was introduced for simultaneous detection of CN^- and ClO^-.

►**2TM** exhibits excellent selectivity, great sensitivity and ultrafast responses to CN^- and ClO^-.

►The low detection limits for CN^- and ClO^- were obtained as 0.96 μM and 48 nM.

►**2TM** sensitively detect CN^- and ClO^- in live cells, water and food samples.

►**2TM** is applied as an efficient sensor for highly colorimetric detection of CN^- and ClO^- on test strips and silica.

Conflict of interest statement

The authors declare no competing financial interest.